Printed in U.S.A.

71-GT-40

an ASME publication

$2.00 PER COPY
$1.00 TO ASME MEMBERS

Investigation Concerning the Fluid Flow in the Mixed-Flow Diffuser

SHINJI HONAMI

KEIZO TSUKAGOSHI

Graduate Course,
Faculty of Engineering,
Keio University,
Tokyo, Japan

TOSHIMICHI SAKAI

Associate Professor,
Tokyo Institute of Science,
Tokyo, Japan

ICHIRO WATANABE

Professor,
Faculty of Engineering,
Keio University,
Tokyo, Japan
Mem. ASME

Velocity profile measurements were performed on the flow in a mixed-flow diffuser with walls having equal cone angles. The aim of the present study is to understand the flow behavior and the relation between the flow patterns and the diffuser losses. The boundary layer flow accompanied by separation on the inner wall and the velocity normal to the diffuser walls were measured in detail to examine the three-dimensional flow behavior in the mixed-flow diffuser. Comparing with the radial diffuser, the mixed-flow diffuser had a more complicated flow mechanism as it had the pressure gradients of transverse and normal directions.

Contributed by the Gas Turbine Division of The American Society of Mechanical Engineers for presentation at the Gas Turbine Conference & Products Show, Houston, Texas, March 28-April 1, 1971. Manuscript received at ASME Headquarters, December 14, 1970.

Copies will be available until January 1, 1972.

Investigation Concerning the Fluid Flow in the Mixed-Flow Diffuser

SHINJI HONAMI KEIZO TSUKAGOSHI TOSHIMICHI SAKAI ICHIRO WATANABE

INTRODUCTION

Recently, many studies concerning mixed-flow compressors have been reported. The flow mechanism within the mixed-flow impeller was investigated by J. D. Stanitz, J. T. Hamrick, F. Dallenbach, and present authors. The researches on the performance of mixed-flow diffusers have been reported by several authors (1),[1] but those on the flow mechanism in the mixed-flow diffuser seem to be unavailable. On the other hand, many studies on the performance and the flow mechanism of vaneless radial diffusers have been performed (2-5).

The main factors, which influence the losses in the diffuser, are as follows.

1 The boundary-layer development on the diffuser walls. Conventional loss analyses for the radial diffuser (6,7) were assumed a one-dimensional flow, and the wall friction factor was taken as a function of the diffuser radius. W. Jansen (8) developed the skewed boundary-layer theory over the one-dimensional analysis, assuming the inlet flow to be a steady, axisymmetric, and symmetric one with respect to the mid-plane.

2 The asymmetric flow caused by the wakes of the impeller. R. C. Dean and Y. Senoo (9) developed the analysis to account for the jet and wake mixing loss produced by the rotating wakes shed from the compressor impeller.

3 The unsymmetric flow with respect to the mid-plane between the two walls.

4 Three-dimensional effects of the mixed-flow diffuser. A parallel-walled radial diffuser consists of two flat plates, but a mixed-flow diffuser has two conical surfaces; the inner surface is formed by a convex surface and the

[1] Underlined numbers in parentheses designate References at end of paper.

NOMENCLATURE

c_f = wall friction factor

b = diffuser width

n = distance from the inner wall

n^* = streamline coordinate (Fig.3)

p = static pressure

R^* = radius of curvature

r = radius

R = radius ratio $(=r/r_i)$

Re = Reynolds number

U = absolute velocity of main flow

u, w = velocity components in boundary layer parallel and normal to main flow, respectively (Fig.3)

V = velocity

V_θ = tangential component of velocity

V_m = meridional component of velocity

V_n = normal component of velocity to diffuser walls (positive in direction of increasing n)

β = flow angle between mid-plan and resultant velocity vector. The positive value corresponds to the angle in the case of resultant velocity vector being directed toward outer wall.

γ_w = angle between wall shear stress vector and main flow direction

θ = flow angle from tangential direction

ρ = density

Subscripts

i = inlet of diffuser

1 = normal direction to streamline in plane parallel to diffuser walls (direction of principal normal) (Fig.3)

2 = normal direction to streamline in plane normal to diffuser walls (direction of bi-normal) (Fig.3)

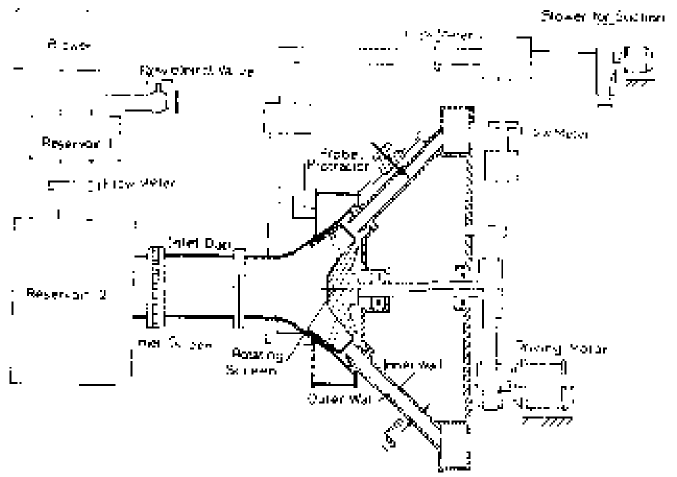

Fig.1 Experimental set arrangement

outer surface by a concave one.

In addition to the foregoing factors, other effects, caused by the turbulence and so on, are considered.

In the present paper, the aforementioned factors, except item 2 were investigated with special reference to item 4.

EXPERIMENTAL ARRANGEMENT

A schematic drawing of the entire apparatus is given in Fig.1. In the inlet duct, two screens with 60 mesh/sq in. were installed to suppress the turbulence. Two rotating screens of 60 mesh in front of the diffuser inlet were installed to give the air a tangential component. Knife-edged diffuser inlet was employed. The mean radius of the diffuser inlet measured from the rotating axis amounted to 100 mm. In order to control the inlet flow patterns, suction devices were installed. The distance between the inner and outer diffuser walls was kept constant at 18 mm. The pressure and turbulence level measurements were conducted at various radius ratios. To make precise measurements near the inner wall, the probe was inserted from the outer wall. The protractor was used to measure the direction of flow within the diffuser from the tangential direction. A traverse measurement of the inner wall boundary layer was conducted by a dial gage having an accuracy of 0.05 mm. Further, the velocity normal to the diffuser walls and the turbulence levels were measured. A reading microscope, having a vertical scale range of 150 mm with a reading accuracy of 0.05 mm, was used in observing the water manometer which indicated the pressure difference of a cobra probe, and a protractor having an accuracy of 0.1 degree with a vernier was employed for determination of the flow angle by nullifying the pressure difference of two side holes of the probe.

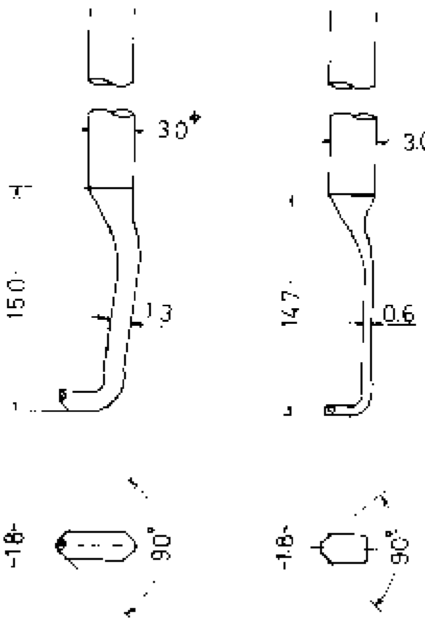

Fig.2 Probes

The traverse of a four-hole cobra probe (Fig.2) was conducted merely in the regions where it is permissible to neglect the wall effects, i.e., more than 4 and 3 mm apart from the inner and the outer walls, respectively. The four-hole cobra probe was employed to investigate the shift of the main flow toward the outer wall, in view of the shift phenomenon of the main flow recognized in the preliminary experiment. For the turbulence measurement, a constant temperature hot-wire anemometer was adopted.

Inlet flow angle, θ_1, was varied by setting the flow rates from 0.16 to 0.22 kg/sec at the constant rotational speed of screen of 3240 rpm. The flow rate was measured by a standard nozzle placed between the two reservoirs, and the rotational speed was measured by an electromagnetic digital counter. The Reynolds number based on the diffuser inlet conditions amounted to

$$Re = \frac{h\ V_1}{\nu} \cong 3.1 \times 10^4$$

where h was the diffuser width and V_1 was the inlet flow velocity. A fully turbulent boundary layer was revealed by adverse pressure gradient and through measurements of the turbulence level.

INLET FLOW CONDITION

The diffuser loss of a vaneless diffuser is influenced by the condition of the flow at the inlet. If a set of stationary vanes at the diffuser inlet is employed to give a tangential velocity component to the fluid, wakes shed from

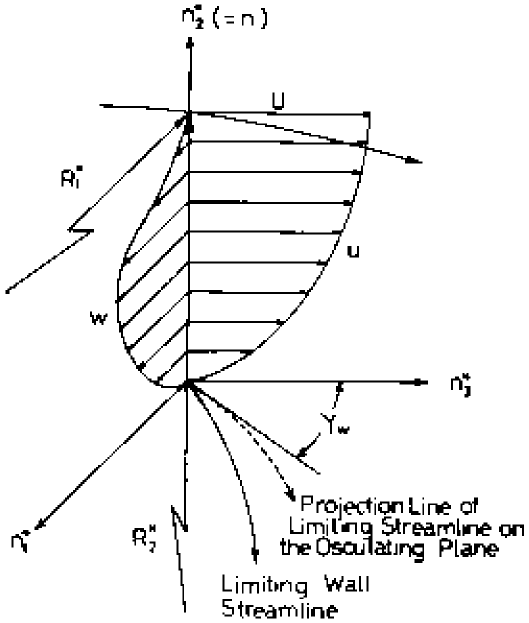

Fig.3 Typical three-dimensional boundary layer and its coordinates

the stationary vanes are formed, thus extending all the way to the diffuser exit and producing an asymmetric flow. In the case of a rotating impeller, rotating wakes generate wake mixing losses, but the wakes disappear more rapidly near the diffuser inlet than from the stationary vanes.

To exclude the aforementioned influence, in the present study, a rotating screen was installed to give the fluid a tangential component at the inlet.

Three flow regimes are conceivable in the diffuser inlet:

1 One-dimensional flow
2 Two-dimensional flow, i.e., the flow in which all the velocity vectors lie on one plane
3 Three-dimensional flow

To investigate the flow model, it is desired to produce the flow of case 1 at the inlet, but it is very difficult to make a one-dimensional flow in the mixed-flow diffuser because of the difference of peripheral velocities between the hub and the shroud of the rotating screen. The distribution of the tangential velocities at the diffuser inlet was not uniform but had a gradient between the two walls.

Through adjustment of suction flow rates at the diffuser inlet and adequate installation of the two screens at the same impeller exit, the flow pattern corresponding to case 2 was obtained. In the present experiments, the outlet conditions generated by the rotating screen attached to the mixed-flow type were found to be more regular compared with the flow shed from the ordinary mixed-flow impeller.

EXPERIMENTAL RESULTS CONCERNING FLOW PATTERN

Three-dimensional measurements of the flow pattern within the mixed-flow diffuser were made. At the inlet of the diffuser, the flow angles in the stream surfaces parallel to the inner and outer diffuser walls were taken at 22 and 17.5 deg. The flow velocity and direction in stream surfaces were determined by a three-hole cobra pitot tube and the three-dimensional flow pattern, except in the vicinity of the diffuser walls was obtained by a four-hole cobra pitot tube. Because of the geometry of the four-hole cobra tube, nonlinearity of calibration curve between pitching angle and pressure difference of the center hole and the bottom hole was found in the calibration procedure, at large negative pitching angle. By this characteristic of the four-hole cobra tube, the flow directed from the outer wall to the inner wall, i.e., the flow having the negative pitching angle exceeding 10 deg, was found less sensitive.

For the purpose of excluding the influence of a flow along the stem of the probe and rendering possible the measurements of the flow patterns across the diffuser walls throughout the entire region, the pressure probes, having a special geometry as shown in Fig.2, were made and employed in the present experiment.

As mentioned previously, the present authors have endeavored to keep the flow angle distribution between the inner and the outer walls constant at the inlet.

The velocity components (V_θ and V_m) and the flow angle (θ_1) measured by the three-hole pitot tube are shown in Figs.4 and 5. The slope of the meridional velocity component (V_m) at the inlet was abandoned to have a slight gradient because of the difference of the tangential velocity component due to peripheral velocity differences at screen outlet. As the radius ratio increased, the slope of V_m increased rapidly. The tangential velocity (V_θ) had also a slight gradient at the inlet because of the peripheral velocity difference as mentioned before. With an increasing radius ratio, V_θ profile became flat. This indicates that the angular momentum tends to be conserved downstream in spite of the forced vortex at the inlet.

In the case of inlet flow angle, 22 deg, the velocity component normal to the walls, V_n, at R = 1.0, directed toward the inner wall, was higher near the outer wall than near the inner

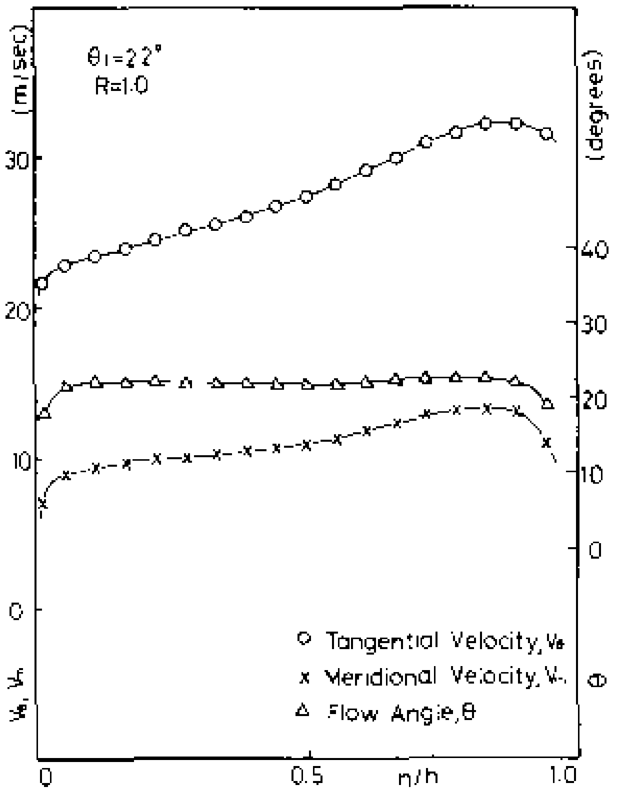

Fig.4(a) Distributions of velocities and flow angles, θ_i = 22 deg, R = 1.0

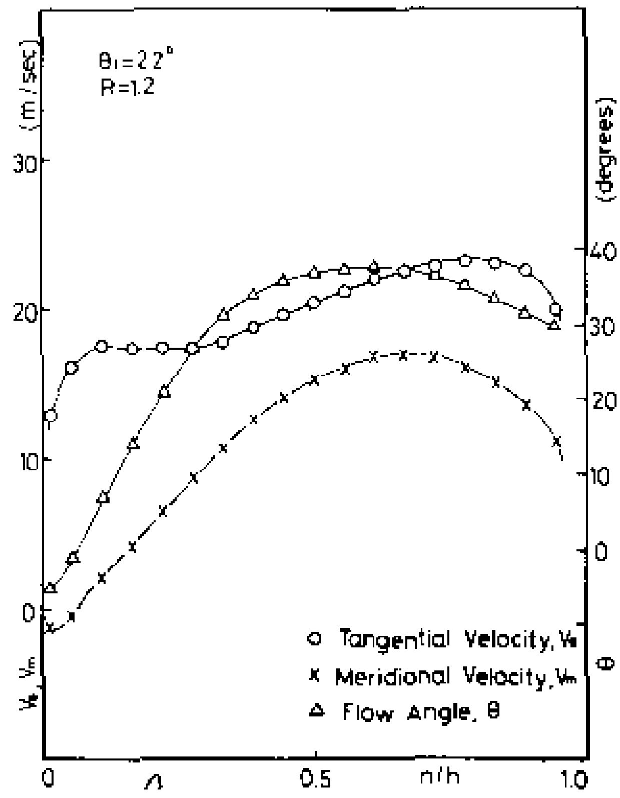

Fig.4(b) Distributions of velocities and flow angles, θ_i = 22 deg, R = 1.2

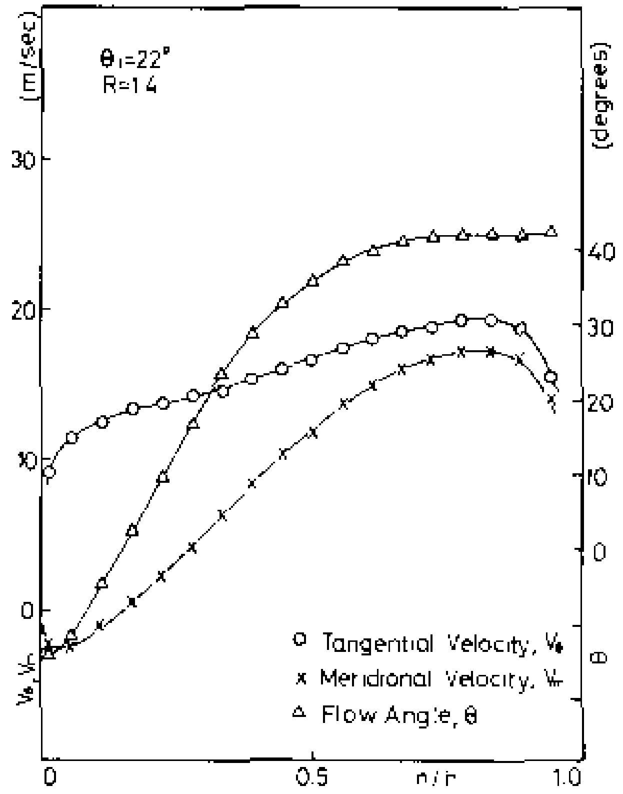

Fig.4(c) Distributions of velocities and flow angles, θ_i = 22 deg, R = 1.4

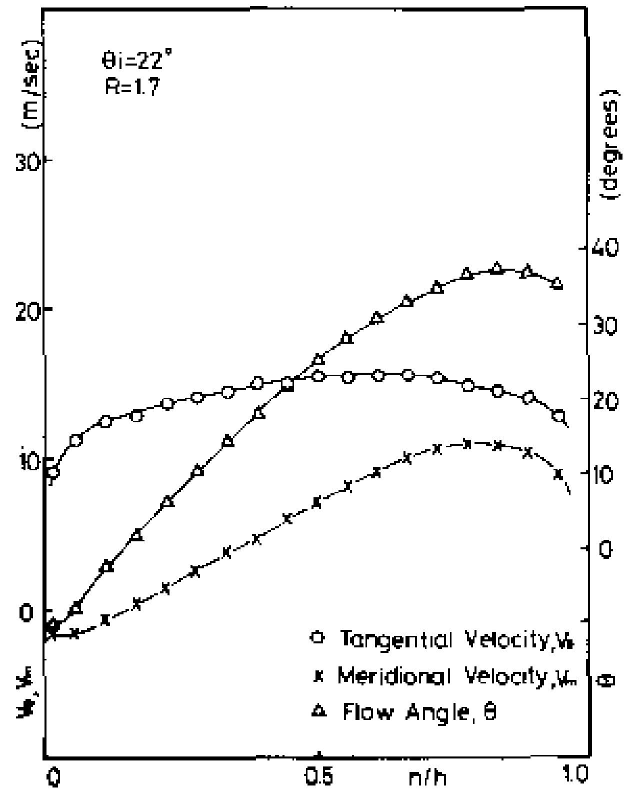

Fig.4(d) Distributions of velocities and flow angles, θ_i = 22 deg, R = 1.7

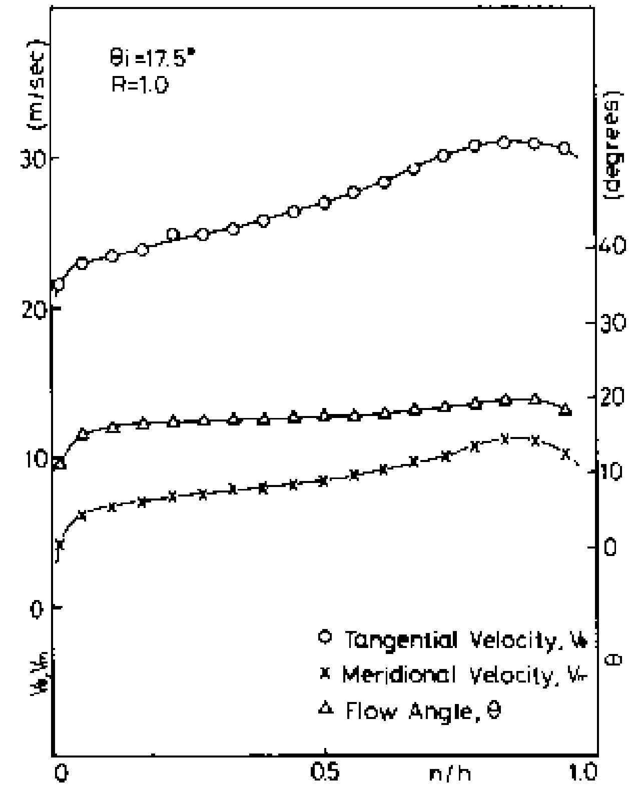

Fig.5(a) Distributions of velocities and flow angles, θ_i = 17.5 deg, R = 1.0

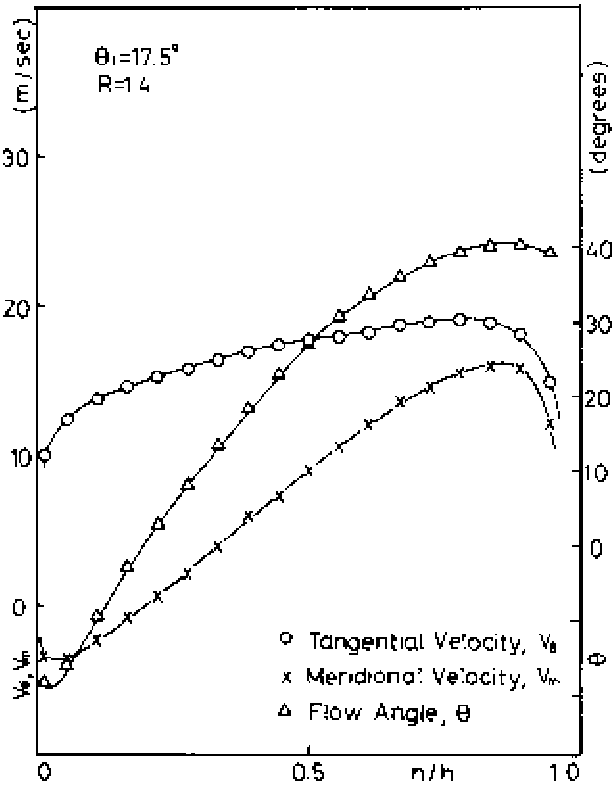

Fig.5(c) Distributions of velocities and flow angles, θ_i = 17.5 deg, R = 1.4

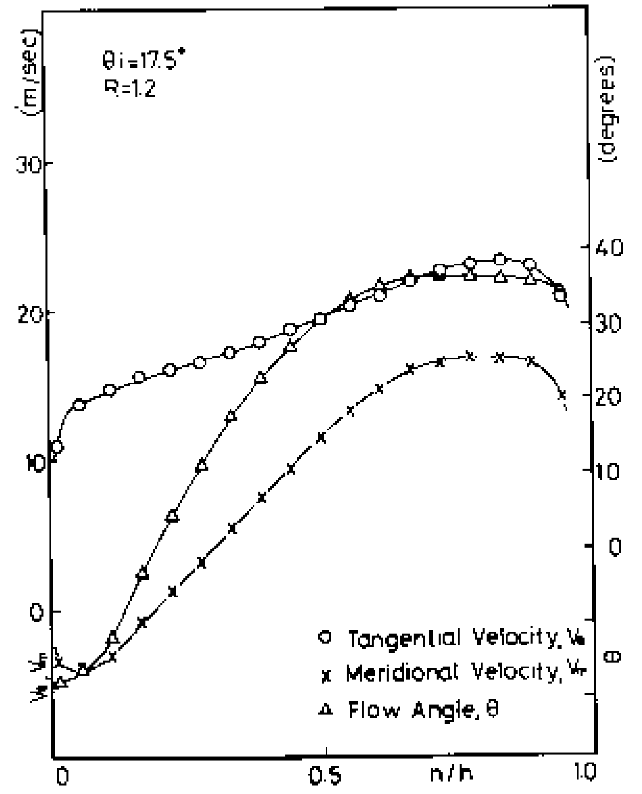

Fig.5(b) Distributions of velocities and flow angles, θ_i = 17.5 deg, R = 1.2

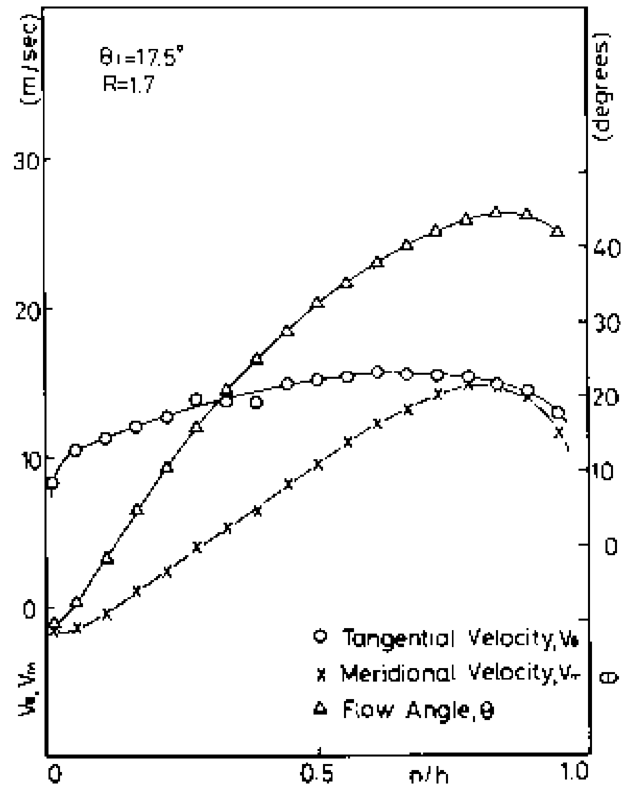

Fig.5(d) Distributions of velocities and flow angles, θ_i = 17.5 deg, R = 1.7

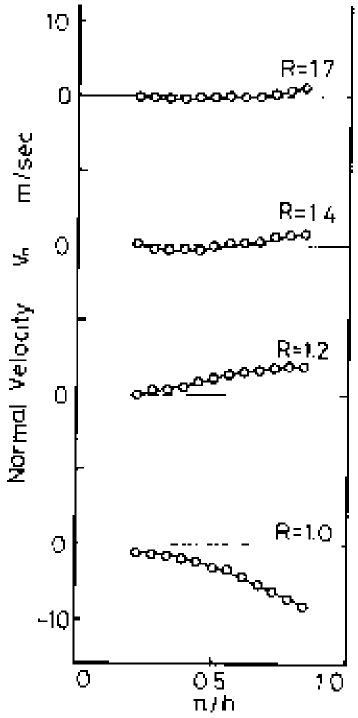

Fig.6(a) Velocity profiles normal to walls, θ_i = 22 deg

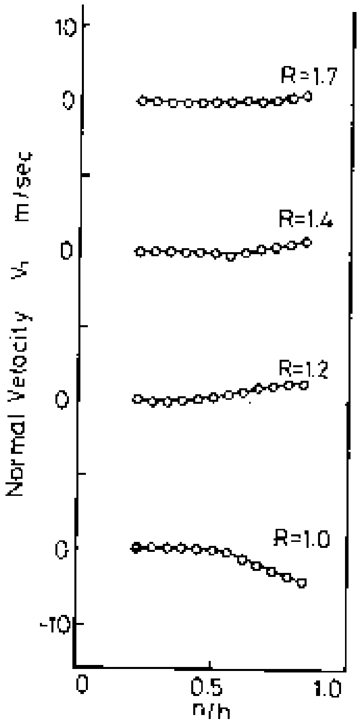

Fig.6(b) Velocity profiles normal to walls, θ_i = 17.5 deg

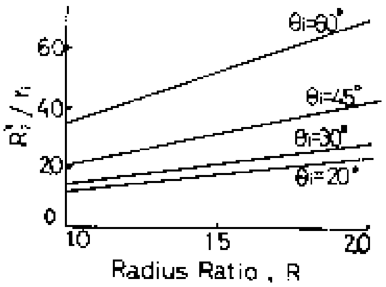

Fig.7 Dimensionless radius of curvature versus radius ratio for inlet flow angle

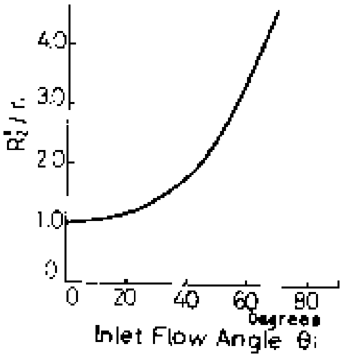

Fig.8 Dimensionless radius of curvature versus inlet flow angle

wall as shown in Fig.6. At inlet flow angle, 17.5 deg, however, V_n at R = 1.0 was almost zero near the inner wall and had a negative value in the region ranging from the mid-pitch to the outer wall. Nevertheless, V_n component tended to have a positive value with an increasing radius ratio. This indicates that in the mixed-flow diffuser, the main flow shifts toward the outer wall under the centrifugal force normal to the wall.

The general tendency in the present investigation revealed that a considerable boundary-layer development took place on the inner wall. On the inner wall, regions of separation were observed to exist and extend all the way to the large radius ratio. With an increasing inlet flow angle, the generation of a region of flow separation was shifted downstream in the present experiment. Thus, in the mixed-flow diffuser, it was found that this type of separation would be generated more easily than in the case of a radial diffuser. In case of radial diffuser, reduction of losses due to flow separation with increasing flow angle was found for small value of b/r, as shown in the paper by Sänger (10). This type of separation corresponds to the "bubble" designated by E. C. Maskell (11).

FLOW IN THE BOUNDARY LAYER

The boundary layer at the inner wall in the

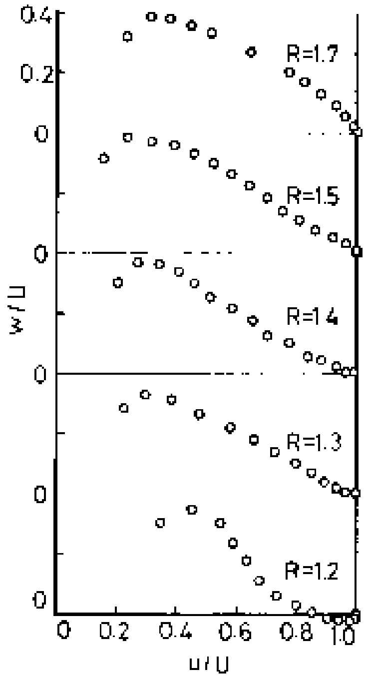

Fig.9(a) Velocity polar plots, θ_1 = 22 deg

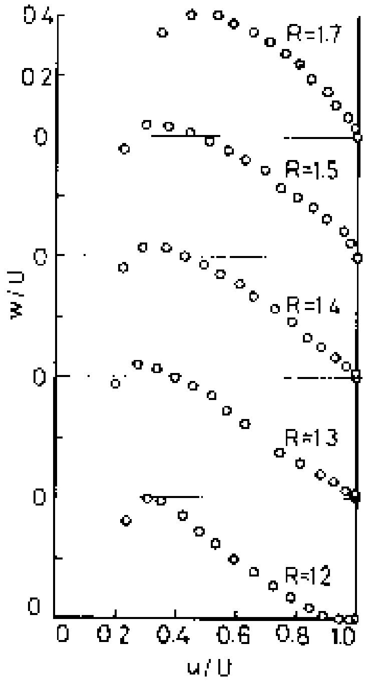

Fig.9(b) Velocity polar plots, θ_1 = 17.5 deg

mixed-flow diffuser was a skewed one in which the velocity vectors were not collateral. These phenomena occur in the radial vaneless diffuser by the mechanism of a secondary flow. The static pressure field is determined by the main flow.

The two components of the pressure gradient normal to the streamline on the mixed-flow diffuser are:

$$\frac{\partial p}{\partial n_1^*} = \rho \frac{V^2}{R_1^*} \qquad (1)$$

$$\frac{\partial p}{\partial n_2^*} = \rho \frac{V^2}{R_2^*} \qquad (2)$$

where suffix 1 indicates the normal direction to the streamline in the plane parallel to the diffuser walls, suffix 2 denotes the normal direction to the streamline in the plane normal to the diffuser walls, R* is the radius of the curvature, and n* denotes its direction as shown in Fig.3. In the radial diffuser, R_2^* is infinite, but R_2^* in the mixed-flow diffuser has a finite value. A relation between R_2^* and the inlet flow angle for a free vortex flow within the mixed-flow diffuser, having a 90-deg cone angle, is shown in Figs.7 and 8.

$$\frac{R_2^*}{r_1} = \frac{2 \tan^2 \theta_1 + 1}{\sqrt{\tan^2 \theta_1 + 1}} \cdot R \qquad (3)$$

The pressure gradient, derivable from equations (2) and (3), is influenced strongly at small inlet flow angle and small radius ratio. From Fig.8, one finds that the pressure gradient at the inlet for the inlet flow angle, 20 deg, is three times as large as that for 60 deg. This pressure gradient between the diffuser walls was also recognized in the present experiment. Thus, it is seen that the static pressure field has a structure having two pressure gradients — one is the adverse pressure gradient in a conventional radial diffuser, the other being this type of gradient, aforementioned.

In the mixed-flow diffuser, it is conceivable that the increment of the static pressure downstream in the midstream plane is smaller than that on the inner surface, due to the increasing radius of curvature of the stream surface downstream. On the other hand, the difference of the increment of static pressures in the radial diffuser is the same on every stream surface. The flow field is influenced through the mechanism shown in equation (1) in the case of a mixed-flow diffuser, as well as a radial diffuser. V in the boundary layer is smaller than the main stream velocity, while the pressure gradient in the downstream direction in the main stream is less than that in the boundary layer. Therefore, the radius of curvature of a boundary-layer streamline must be less than the radius of curvature of the main flow streamline according to equation (1), and it must also be less than the radius of curvature of the boundary-layer streamline in the radial dif-

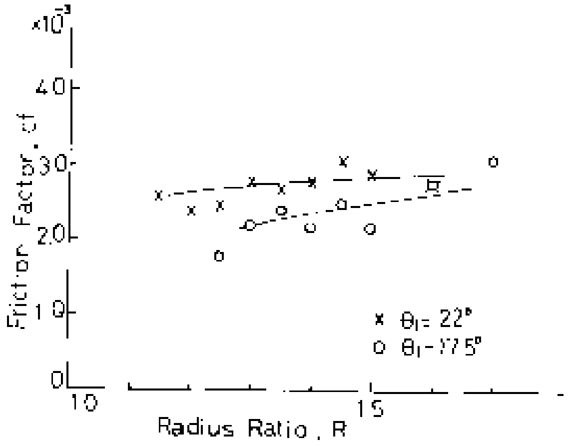

Fig.10 Friction factor of inner wall

face. The difference in direction and magnitude of stream velocities in the boundary layer, as well as in the main stream, yields a large velocity component of a cross flow as shown in Fig.9, and thus, in the mixed-flow diffuser, the skewed boundary layer will be more pronounced than in the radial diffuser. In the mixed-flow diffuser, the radius of curvature of main flow stream (principal normal direction) increases with an increasing radius ratio. The boundary-layer development is much more complicated by the facts that in radial diffusers the cross flow increases downstream, but in mixed-flow diffusers, the increasing cross flow downstream will diminish with the decreasing influence of radius of curvature.

The polar plots concerning u/U versus y/δ in the region from the inner wall to the main stream were employed to evaluate the wall friction factor, Fig.9. The wall friction factor, C_f, of the inner wall was determined from Clauser's "Law of the Wall," modified by J. P. Johnston (12-14).

According to the general relation between the boundary-layer development on the convex surface and the radius of curvature of its surface, the boundary layer becomes thick with a decreasing radius of curvature, and, therefore, the velocity gradient normal to the surface will be small and the wall friction factor will diminish. Taking into consideration the convex and the concave walls, the boundary-layer development at the concave wall will be less than at the convex wall. Fig.10 shows the relation between C_f of the inner wall and the radius ratio. Although the wall friction is an important factor for the diffuser losses and the value generally determines the diffuser performance, as discussed before, it is very difficult to consider the wall friction factor in the mixed-flow diffuser constant as in the case of a radial diffuser and to define the performance in terms of the wall friction factor even if the wake mixing losses are negligible, because the wall friction factor seems to have different values at the inner and the outer walls due to difference of boundary-layer development on each wall.

TURBULENCE LEVEL

In order to completely specify the flow mechanism in the diffuser, it will be necessary to measure not only the time-averaged velocity profile, but also the turbulence in the flow, i.e., three components of turbulent fluctuations and the frequency distributions of turbulence energy if available.

The turbulence measurements made in the present experiment, however, do not give a complete picture, because of lack of measurements concerning the three components of turbulence fluctuation and turbulence energy. The present purpose is to specify the experimental conditions, rather than to clarify the structure of turbulence.

The probe used is constructed of a 2.90-mm-dia porcelain stem and two piano wire needles fitted to the stem supporting a tungsten wire having 0.005-mm dia between them. Only one component of the turbulence intensity, parallel to the average velocity direction, was measured at the sites having various radius ratios, by inserting the hot wire perpendicular to the direction of the average velocity determined previously by the three-hole cobra pitot tube. All traverse measurements were made with the probe inserted through the outer wall.

The results of turbulence intensity surveys in the diffuser are presented in Fig.11. The most significant feature of these results lies in the fact that the turbulence level increases at large radius ratios. At the inlet in spite of being immediate downstream of the rotating screen, however, the turbulence intensity near the walls was higher than that at the main flow. The region of high level coincided with that of the boundary layer. This indicates that turbulence may be generated in the boundary layer. The present authors, however, cannot estimate in detail the manner in which the turbulence energy produced in the boundary layer, as well as how its dissipation contributes to the diffuser losses. It is conceivable that the diffuser loss will be reduced when the turbulence level is suppressed.

CONCLUSIONS

The following conclusions were drawn from the present investigation concerning a mixed-flow diffuser under the condition of the inlet flow having uniform flow angles.

1 The boundary-layer development on the inner wall was more complicated as the main flow shifted toward the outer wall rapidly.

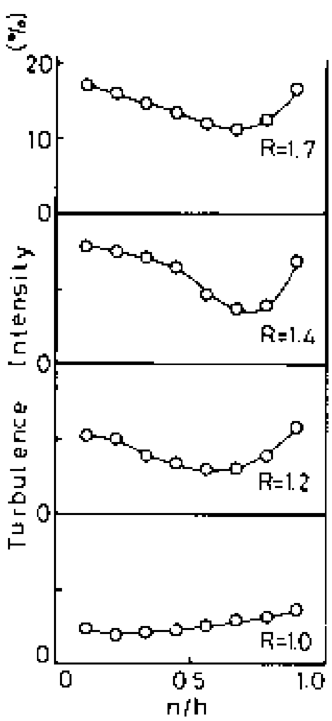

Fig.11(a) Turbulence distributions, θ_i = 22 deg

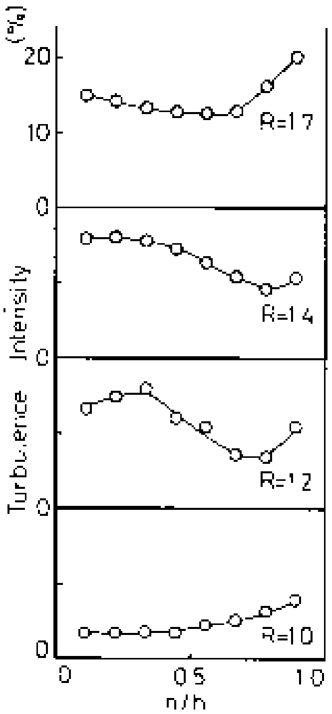

Fig.11(b) Turbulence distributions, θ_i = 17.5 deg

2 The boundary layer on the inner wall was a three-dimensional one. Its skewedness was more remarkable than in the radial diffuser because of the wall curvature.

3 In the mixed-flow diffuser, the flow yielded a pressure gradient normal to the diffuser walls. From the theoretical considerations, it was found also, for example, that the pressure gradient at the inlet for the inlet flow angle, 20 deg, was three times as large as that for 10 deg.

4 In the downstream, the velocity of positive component normal to the walls was found in the main stream, but in the boundary layer, V_r was almost zero.

5 The wall friction factor in the inner wall tended to increase gradually in the downstream direction in case of θ_i = 17.5 deg. In case of θ_i = 22 deg, it seemed to increase slightly or remain almost constant.

REFERENCES

1 Brown, W. B., and Bradshaw, G. R., "Method of Designing Vaneless Diffusers and Experimental Investigation of Certain Undetermined Parameters," NACA TN 1426, 1947.

2 Gardow, E. B., "The Three-Dimensional Turbulent Boundary Layer in a Free Vortex Diffuser," MIT Gas Turbine Laboratory Report No. 42, 1958.

3 Johnston, J. P., and Dean, R. C., Jr., "Losses in Vaneless Diffusers of Centrifugal Compressors and Pumps," Journal of Engineering for Power, Transactions of ASME, Vol. 88, 1966.

4 Ellis, G. O., "A Study of Induced Vorticity in Centrifugal Compressors," Journal of Engineering for Power, Transactions of ASME, Vol. 86, 1964.

5 Mates, R. E., "Three Dimensional Flow in the Diffuser of a Mixed Flow Compressor," Ph.D. thesis, Cornell University, 1963.

6 Stanitz, J. D., "One-Dimensional Compressible Flow in Vaneless Diffusers of Radial and Mixed-Flow Centrifugal Compressors," NACA TN 2610, 1952.

7 Brown, W. B., "Friction Coefficients in a Vaneless Diffuser," NACA TN 1311, 1947.

8 Jansen, W., "Steady Flow in a Radial Vaneless Diffuser," Journal of Basic Engineering, Transactions of ASME, Vol. 82, 1960.

9 Dean, R. C., Jr., and Senoo, Y., "Rotating Wakes in Vaneless Diffusers," Journal of Basic Engineering, Transactions of ASME, Vol. 82, 1960.

10 Sürgel, G., "Untersuchungen am schaufellosen und beschaufelten Diffusor einer Radialgebläsestufe," Maschinenbautechnik, Vol. 17, 1968.

11 Maskell, E. C., "Flow Separation in Three-Dimensions," Report No. Aero 2565, Royal Aircraft Establishment, Farnborough, Nov, 1955.

12 Clauser, F. H., "Turbulent Boundary Layers in Adverse Pressure Gradients," Journal of the Aeronautical Science, Vol. 21, No. 2, 1954.

13 Johnston, J. P., "Three Dimensional Turbulent Boundary Layer," MIT Gas Turbine Laboratory Report No. 39, 1957.